Interpretation of ria tests. Buckling of fuel plates

J.-M. Gatt

INTERPRETATION OF RIA TESTS. BUCKLING OF FUEL PLATES

Jean-Marie GATT

Engineer, CEA, France

ABSTRACT

This paper presents an interpretation of transient experiments using a low enriched uranium silicide miniplate fuels prepared for the Japan Research Reactor-3. These tests were performed for the Nuclear Safety Research Reactor (NSRR) at Japan Atomic Energy Institute (JAERI). The miniplates are submitted to power pulses to simulate RIA accident. According to the deposited energy, a geometrical instability can be observed. In the first part of this paper, the methods by eigen modes and perturbation are presented in the framework of the study of a shell in thermal compression. In the second part a description of the tests will be performed. Different approaches to interpret these tests, using finite elements and an analytical approach will be presented. The first approach uses the Eigen modes. To take into account the geometrical defects of the plate, we propose to use a perturbation method. The defects are modelled using the first Eigen mode. These two approaches assume an elastic behaviour of the structure. To take into account of the plasticity, a perturbation method is used. The different experimental results, as the buckling temperature and the final shape of the plate, are found.

INTRODUCTION

This paper presents an interpretation of power transient experiment (RIA: Reactivity Initiated Accident) using a low enriched uranium silicide and aluminide miniplate fuel. This kind of fuel is used in the research reactors. The power pulses were carried out in Nuclear Safety Research Reactor (NSRR) at Japan Atomic Research Institute (JAERI) between 1991 and 1995 [1][2][3]. Above 390°C, the buckling of the miniplate can be observed. In the first part of this paper, the methods by eigen modes and perturbation are presented in the framework of the study of a shell in thermal compression. In the second part the tests and observations are presented. In the third part, these methods are used to simulate, in the elastic domain, the miniplate behaviors. In the fourth part, an application in the plastic domain is proposed and compared to experimental results. Finally in the last part an analytical approach is proposed to check the trends of numerical simulations.

THE SHELL BUCKLING

The buckling of a shell can be studied from three approaches: analytical, eigen modes and perturbation.

Analytical approach and eigen modes

In the elastic domain, there is an analytical solution for the shell buckling [4]. The shell is embedded (the radial dilatation is allowed) between two walls and heated. The critical temperature reads:

$$\Delta T_c = \frac{e}{\alpha R\sqrt{3(1-\nu^2)}} = 904\,°C$$

With e the thickness of the shell: 1.37 mm, R the radius: 41 mm, α the thermal dilatation: 22.6 10^{-6} K^{-1} and ν the Poisson coefficient: 0.33

The eigen mode method gives a critical temperature of 900°C (error 0.4%).

Perturbation approach

The approach consists to take into account some geometrical defects in the structure. This method can be decomposed in tree steps:

1. Performing a finite elements calculation to obtain the first eigen mode.
2. Using the normalized deformation of this mode multiplied by the maximal size of the defect (Figure 2).
3. Performing a finite elements calculation on this pre-distorted structure.

The last step must be performed using a special numerical method: driving in strain. If the strain increment is upper that a criteria (0.5% for example) the time step must be divided by a factor. This process allows detecting the bifurcation point, when the structure buckling starts. Of course, we must take into account large deformations of the structure after the bifurcation. The results of these calculations with different defect sizes (10^{-3}, 10^{-4} and 5.10^{-5} mm) are shown in the Figure 3. The more the defect is small and the more the solution converges toward analytical solution and eigen mode solution.

TESTS AND RESULTS PRESENTATION

These tests performed in the NSRR were carried out by JAERI to study fuel miniplates behavior (made with an aluminide border and a meat aluminide/U_3Si_2) submitted to speed power pulse (during some millisecond) to simulate a RIA. The miniplate sizes are (Figure 1):

- For the meat (mm) : 70 length x 25 width x 0.51 thickness
- For the cladding (mm) : 130 length x 35 width x 0.38 thickness

The meat was made of U_3Si_2 particles in A5 (French standard) matrix. The cladding was made of AG3 (French Standard). These tests highlight four different behaviors according to the power and therefore the plate temperature:

- At low temperature, the plate was stable with no significant damage
- When the temperature increases the crack appears, but the dimensional stability remained good
- At higher temperature a buckling of the plate is observed
- the plate is molten, when the melting temperature is reached

There are seven thermocouples **(**Figure 1) on the active part of the plate (part including meat and cladding) and two on the cladding out of active part. The first crack appeared for a mean cladding temperature of 207±18°C. The buckling is activated for a mean cladding temperature of 418±74°C. For a mean temperature lower than 391 °C (no incertitude) there is no buckling. A partial melting is observed for some plates when the temperature is above 640°C (melting temperature of aluminum).

BUCKLING OF THE PLATE

The maximum temperature of the plate is reached after 50 milliseconds. The temperature rate is very important. This remark allows considering a plastic behavior of the plate. The viscoplastic behavior is negligible. Further, the thermic gradient through the thickness of the plate is also neglected. Indeed, the temperature of the active part of the plate is considered uniform. Furthermore, the temperature of the border (out of the active part) is assumed constant, equal to room temperature. A simple calculation of time constant $t = \frac{L^2}{a} = 380\ ms < 50\ ms$ (the water is not considered, so this time is undervalued) allows showing that the frame stays to constant temperature. With: “a” the thermal diffusivity and “L” the length of frame (5 mm).

The active part of the plate, made with tree layers, is considered uniform. Its properties are evaluated by homogenization (see below).The meshing of the plate is showed Figure 4. The finite element used is quadratic (20 nodes). This meshing is optimized for a good accuracy with a reasonable calculation time. One side of the plate is embedded. At t_0 the temperature is assumed uniform equal to 20°C. The temperature increases up to a maximal temperature. The frame is maintained cold (20°C). The temperature increment imposed to the plate is:

$$\Delta T(°C) = T_{max} - 20$$

Elastic analysis

The high temperature reached by the plate induced a plastic behavior. Therefore, the goal of this elastic analysis is to compare the perturbation approach and eigen mode method for the plate. This step allows working out the numerical methods for perturbation approach. Indeed, the eigen method can be used as the reference method.

Behavior models

The mechanical behavior is assumed elastic (Young modulus E, Poisson coefficient ν and thermal dilatation α).
For the frame: E_c=70000 MPa, ν_c=0.33, α_c= 23.08.10^{-6} K^{-1}
For the active part ("c" for cladding and "m" for meat):

- E_c=65000 MPa, ν_c=0.33, α_c= 24.2.10^{-6} K^{-1}
- E_m=68100 MPa, ν_m=0.29, α_m= 22.6$10^{-6}$ K^{-1}

The three layers are parallel, neglecting in first order the Poisson coefficient, the following equations can be used to estimate E_{ac} and α_{ac} for the active part [5]:

$$\begin{cases} E_{ac} = \dfrac{2e_cE_c + e_mE_m}{e} \\ \alpha_{ac} = \dfrac{2e_cE_c\alpha_c + e_mE_m\alpha_m}{eE_{ac}} \end{cases}$$

With e_c and e_m the cladding and meat thickness respectively, and e = $2e_c + e_m$ the thickness of the plate. These equations give the following results: E_{ac}=66245 MPa, α_{ac}= 23.6.10^{-6} K^{-1}. The Poison coefficient is: ν_{ac}=0.29

Eigen mode approach

The calculation is performed in two steps. The first consists to perform an elastic calculation of the structure. The second uses a special process in cast3M code which evaluates the buckling eigen modes and the associated eigen values k_i. These values give the multipliers to obtain the critical temperature for different modes. For the first mode:

$$\Delta T_c = k_1 \Delta T$$

The results for the three first modes are showed Figure 5. The buckling temperature for each mode is: 404°C, 506°C and 721°C. The last mode is not physic because the temperature is above the melting temperature. It can be remarked that, this approach gives buckling temperatures close to experimental temperatures.

Perturbation approach

This approach consists in introducing in the structure a defect in the initial geometry. This defect is evaluated with the first mode calculated by the above method, from the eigen mode method. The numerical method used is explicit. Some very small time steps are necessary close to the bifurcation of the plate. For that a control strain is used. This numerical method allows devising the time step if the strain increment is upper than a critical value (5 % for example). Despite this, an optimization between the time step and the meshing must be found to manage the bifurcation and avoid the negative Jacobiens and non-convergence. The calculations are performed for different defect sizes from 1mm to 10µm. The displacement of the plate is evaluated from the following equation:

$$d = \max_{nodes} \sqrt{u_x^2 + u_y^2 + u_z^2}$$

With: $\vec{u}(u_x, u_y, u_z)$ the displacement field of the nodes of the structure.

The Figure 6 shows for each defect the maximal displacement evolution of the plate versus the temperature increment between active part and cold frame. These results are compared to a reference calculation without defects. For a large defect, in order of magnitude of the plate thickness, the bifurcation appears earlier, with a progressive evolution of the displacement of the plate. In opposite, for small defects, the bifurcation appears later with a fast evolution of the plate displacements. The temperature bifurcation is 400°C (ΔT=380°C) for a defect size of 10µm and less for larger defects. This result is in good agreement with eigen mode approach.

PLATIC ANALYSIS

Behavior model

The active part and the frame are assumed to have a linear cinematic plastic behavior. As shown in Figure 7 this model is characterized by two parameters: a hardness (h) modulus and yield stress σ_y.

$$\varepsilon_i = \frac{\sigma_i}{E_i} + \frac{\sigma_i - \sigma_{Yi}}{h} \ with \ \frac{1}{h} = \frac{1}{E'_i} - \frac{1}{E_i}$$

(i=1 for the frame and i=2 for the active part)

The hardening modulus is assume small and the same for both materials (frame and active part)

For the plastic part, the following parameters have been considered.

For the frame: σ_{Y1} = 130 MPa and h = 750 MPa

For the active part, the yield stress is considered as a parameter of this approach:

- σ_{Y2} = 40, 50 and 60 MPa
- h = 750 MPa

Perturbation approach

The perturbation method, in the plastic case, is the same as in elastic case; the difference is only the material behavior. The defect taken into account is evaluated from first eigen mode evaluated in the elastic domain. Its maximal size is 10µm. The whole test has been simulated: temperature increasing up to 420°C and decreasing up to 120°C (from 120°C the temperature decreases lower). The Figure 8, Figure 9 and Figure 10 show the displacement evolution of the plate versus the temperature increment for different levels of temperature (T_{max} = 270°C, 320°C, 370°C et 440°C) and different hypothesis on the yield stress of the active part (40, 50 and 60 MPa). These calculations are compared to a reference calculation without defect at 440°C. The simulations show that the buckling appears during the cooling for a temperature between 370 and 440°C. The temperature range is in good agreement with experimental results. For a temperature increment of 420°C (Figure 8) a bifurcation appears during the temperature increasing. The results depend on the choice of the yield stress. Nevertheless this choice does not modify drastically the order of magnitude of buckling temperature.

ANALYTICAL APPROACH

The analysis proposed below allows confirming with a simplified analytical approach the buckling mechanism observed in the numerical simulations. The axial thermal plate dilatation is free, so in the coordinate system presented in the Figure 11, the longitudinal balance (the stress in "y" direction is negligible) of the plate reads:

$$2L_1\sigma_{x1} + L_2\sigma_{x2} = 0$$

We have: L_1 = 5mm and L_2 = 25 mm. Therefore:

$$\sigma_{x2} = -\frac{2L_1}{L_2}\sigma_{x1} = -0.4\sigma_{x1}$$

The elastic solution of this problem is:

$$\frac{\sigma_{x1}}{E_1} = \frac{\sigma_{x2}}{E_2} + \alpha\Delta T = -0.4\frac{\sigma_{x1}}{E_2} + \alpha\Delta T$$

And then: $\begin{cases}\sigma_{x1} = E^*\alpha\Delta T \\ \sigma_{x2} = -0.4E^*\alpha\Delta T\end{cases}$ $with\ \frac{1}{E^*} = \frac{1}{E_1} + \frac{0.4}{E_2}$

For ΔT = 400°C, the stress in active part equal to: -176 MPa.

During the loading:

The plastic solution of this problem when the active part yielded in first (for ΔT = 400°C and $\sigma_{Y2} = 40MPa$) is:

$$\begin{cases}\sigma_{x1} = \hat{E}_2\left(\alpha\Delta T - \frac{\sigma_{Y2}}{h}\right) = 112MPa \\ \sigma_{x2} = -0.4\sigma_{x1} = -45\ MPa\end{cases} \quad with\ \frac{1}{\hat{E}_2} = \frac{1}{E_1} + \frac{0.4}{E'_2}$$

The plastic solution of this problem when the frame part yielded in first (for ΔT= 400°C and $\sigma_{Y2} = 60MPa$) is:

$$\begin{cases}\sigma_{x1} = \hat{E}_1\left(\alpha\Delta T + \frac{\sigma_{Y1}}{h}\right) = 135\ MPa \\ \sigma_{x2} = -0.4\sigma_{x1} = -54\ MPa\end{cases} \quad with\ \frac{1}{\hat{E}_1} = \frac{1}{E^*} + \frac{1}{h}$$

If we consider the active part as a rectangular plate posed and submitted to uniform compression, the critical buckling stress reads:

Elastic: $\sigma_{cre} = \frac{\pi^2 D}{b^2 e}\left(\frac{\beta}{m} + \frac{m}{\beta}\right)$

Plastic: $\sigma_{crp} = \frac{\pi^2 D}{b^2 e}\left(\frac{\beta}{m} + \frac{m}{\beta}\sqrt{\frac{\bar{E}}{E}}\right)$

With: $\beta = 2.8$ the ratio length to width of the plate, $D = \frac{Ee^3}{12(1-\nu^2)}$ the bending rigidity of the plate, b=70mm the width, e=1.27mm the thickness of the plate, "m" is an integer representing the wave number minimizing $\left(\frac{\beta}{m} + \frac{m}{\beta}\right)$ or $\left(\frac{\beta}{m} + \frac{m}{\beta}\sqrt{\frac{\bar{E}}{E}}\right)$ and $\bar{E} = \frac{4EE'}{\left(\sqrt{E}+\sqrt{E'}\right)^2}$ the Von Karman reduced modulus.

The numerical application gives: $\sigma_{cre} = 512\ MPa\ and\ \sigma_{crp} = 202\ MPa$. These values are certainly underestimated, because in this analysis the cold frame in traction is not taken into account. In any cases, with or without yielding of the active part, the stress stays largely lower than the critical stresses evaluated by analytical approach. Therefore, the buckling can't appear during power increasing, but instead when the power decreases (the temperature decreases).

During the unloading:

Several cases can be studied: If the active part or frame yielded or not during the load, during the unloading: the active part can yield or the frame can yield or the unloading is totally elastic. The most conservative case is when the frame has yielded during the loading and unloading. In this case the solution is:

$$\begin{cases}\sigma_{x1} = \hat{E}_1 \dfrac{\sigma_{Y1}}{h} = -128\ MPa \\ \sigma_{x2} = -0.4\sigma_{x1} = 51\ MPa\end{cases}$$

In the other configurations, the stress in the frame is greater.

The Figure 12 summarizes the behavior in the case where the active part yields during the temperature increase. If the frame is considered as a beam on ball, with the following sizes: (length x thickness) L=70mm, e=1.27 mm. The critical stress reads:

- Elastic: $\sigma_{cre} = \frac{\pi^2 e^2 E}{12L^2} = 18\ MPa$
- Plastic: $\sigma_{crp} = \frac{\pi^2 e^2 E}{3L^2} \frac{1}{\left(1+\sqrt{\frac{E}{E'}}\right)^2} \approx 0\ MPa$

Low values of this estimations show that the plate buckling during unloading is more likely that during the temperature increase. This very simplified approach allows understanding the solutions of numerical simulations.

CONCLUSION

This study allows a better understanding of the results obtained during NSSR tests. Three approaches, in the elastic domain, have been proposed. These methods give the same results. In the plastic domain, the perturbation approach has been used. The simulations, using this method, give results very closed to experimental results. The buckling appears during the unloading of the structure.

REFERENCES

[1] K. Yanagisawa, T. Fujishiro, O. Horiki, K. Soyama, H. Ichikawa, T. Kodaira, 1992, *Dimensional stability of low enriched uranium silicide plate-type fuel for research reactors at transient conditions*, J. of Nuclear Science and Techno., 29 (3), pp 233-243

[2] K. Yanagisawa, T. Fujishiro, O. Horiki, K. Soyama, H. Ichikawa, T. Kodaira, 1993, *Transient behavior of low enriched uranium silicide plate-type fuel for research reactor during reactivity initiated accident conditions*, J. of Nuclear Science and Techno., 30 (8), pp 741-751

[3] K. Yanagisawa, T. Fujishiro, K. Soyama, H. Ichikawa, T. Kodaira, 1994, *Transient behavior of silicide plate-type during reactivity initiated accident conditions*, Jaeri-M 94-042

[4] R ;J ; Roark, W.C. Young, 1976, *Formulas for stress and strain*, 5ème Edition McGraw-Hill Int editions

[5] M. Bornert, T. Bretheau, P. Gilormini, 2001, *Homogénéisation en mécanique des matériaux*, Hermes Science, Vol 1

[6] G.H. Handelman, W. Prager, *Plastic buckling of rectangular plate under edge thrust*, Report 946; National advisory committee for aeronautic.

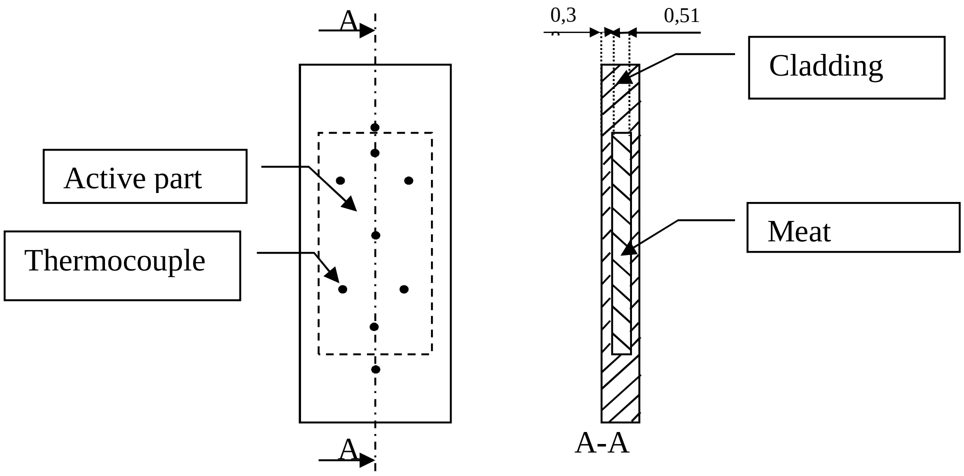

Figure 1: Geometry of the plate

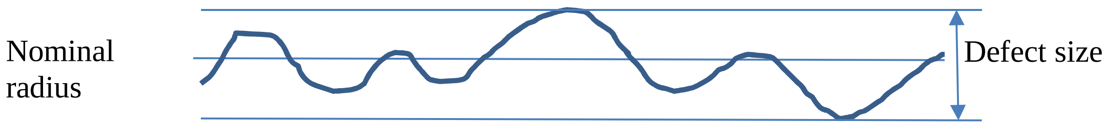

Figure 2 : Defect geometry

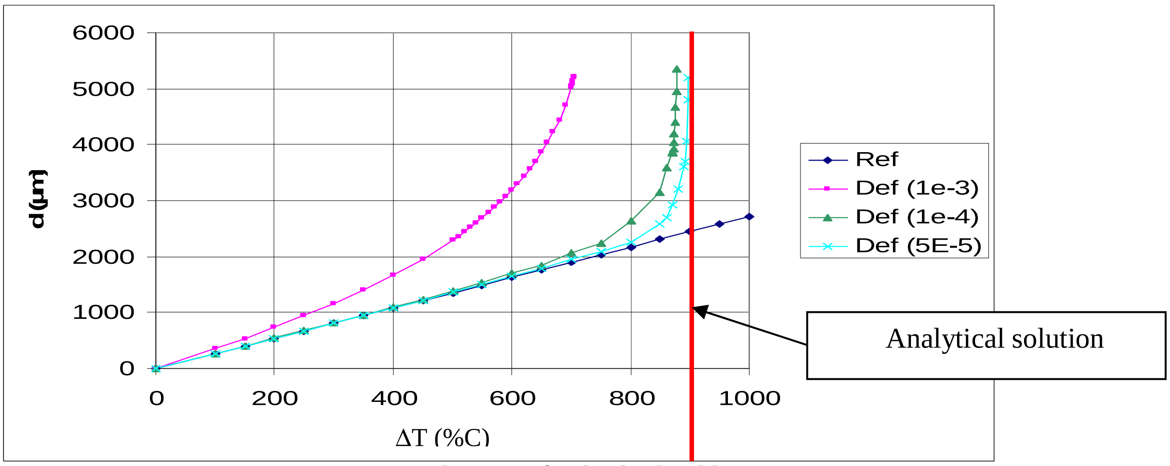

Figure 3 : simulations of cylinder buckling

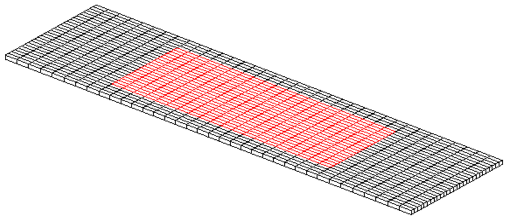

Figure 4: Meshing of the plate

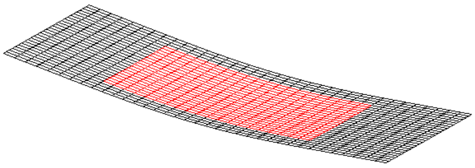

Mode 1 ΔT=404°C

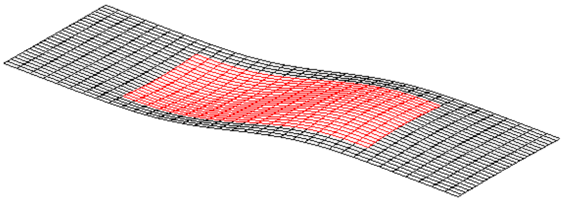

Mode 2 ΔT=506°C

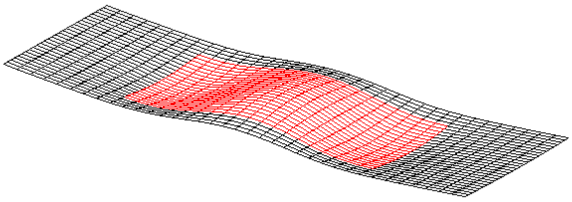

Mode 3 ΔT=721°C

Figure 5: Three first Eigen modes

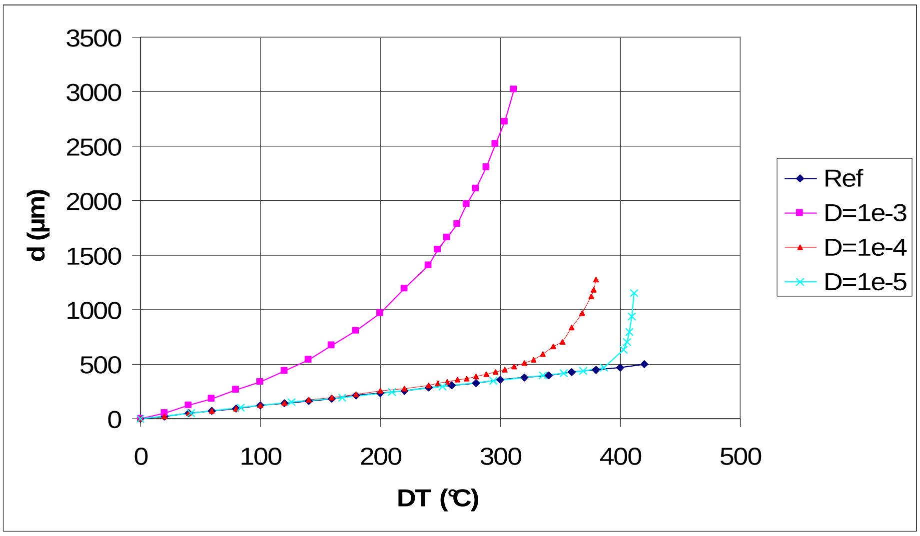

Figure 6: Deformation of the plate for different defect sizes

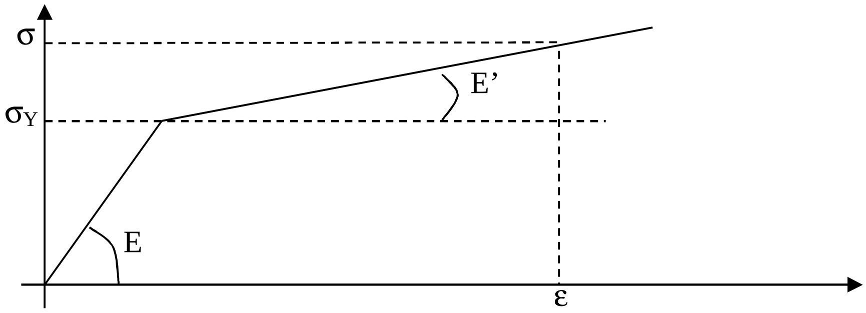

Figure 7: cinematic behaviour model

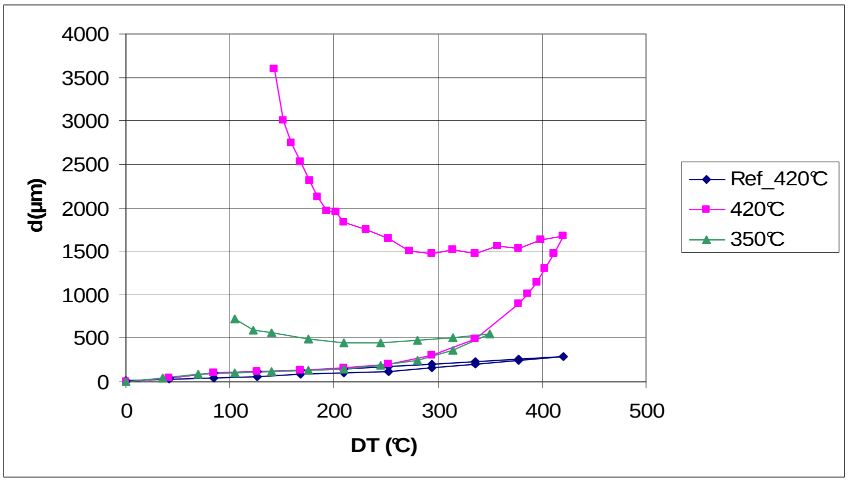

Figure 8: Results from perturbation method $\boldsymbol{\sigma_{Y2} = 40}$ **MPa** and a defect of 10 µm

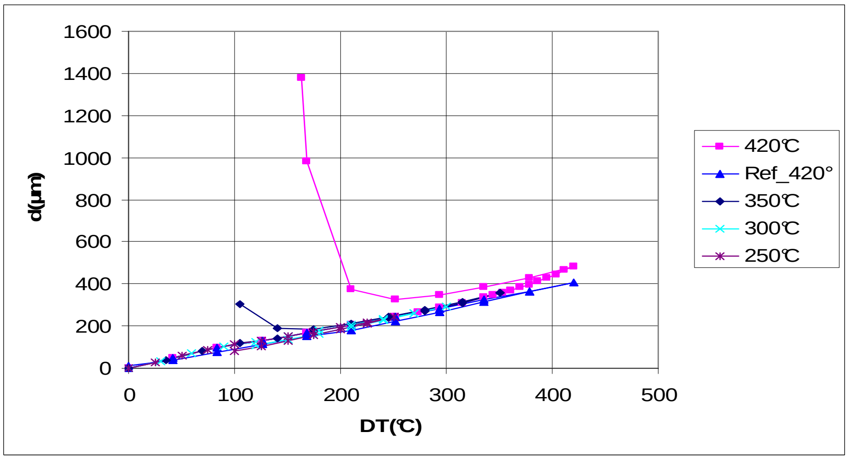

Figure 9: Results from perturbation method $\boldsymbol{\sigma_{Y2} = 50}$ **MPa** and a defect of 10 µm

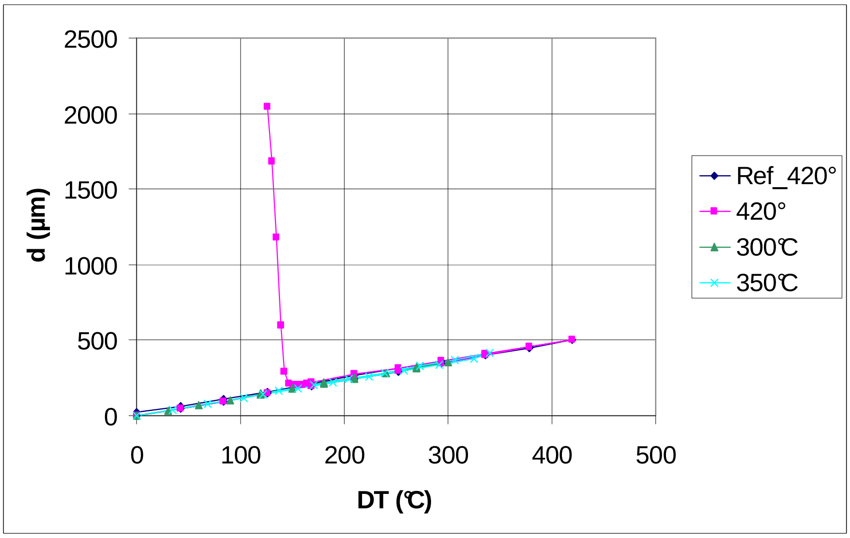

Figure 10: Results from perturbation method $\boldsymbol{\sigma_{Y2} = 60}$ **MPa** and a defect than 10 µm

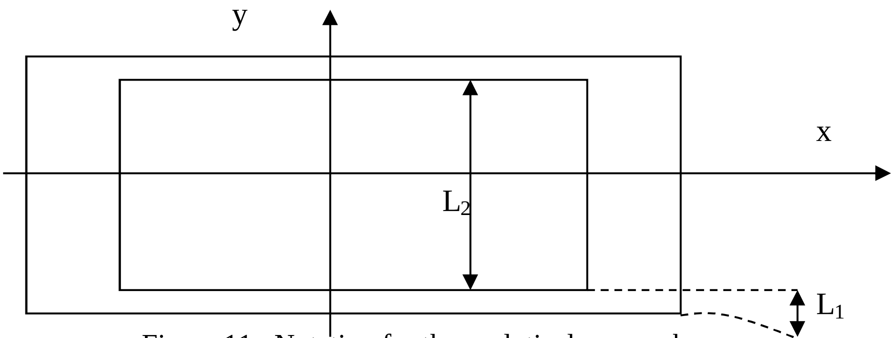

Figure 11: Notation for the analytical approach

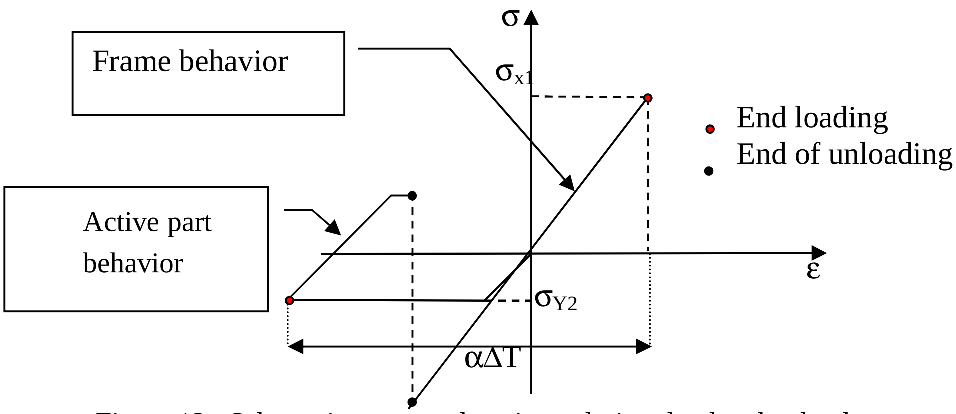

Figure 12: Schematic stress and strain evolution: load and unload